



Multiphase Structures in Case Hardening Steels following Continuous Cooling

H. Roelofs, S. Hasler, L. Chabbi, U. Urlau, [†] J. Chen and [†] H. K. D. H. Bhadeshia

Swiss Steel AG, 6021 Emmenbrücke, SWITZERLAND

[†] *University of Cambridge, Materials Science and Metallurgy, Cambridge CB2 3QZ, U. K.*

New development on metallurgy and applications of high strength steels, Buenos Aires,
26.-28. Mai 2008

Multiphase Structures in Case Hardening Steels following Continuous Cooling

H. Roelofs, S. Hasler, L. Chabbi, U. Urlau, [†]J. Chen and [†]H. K. D. H. Bhadeshia

[†]University of Cambridge
Materials Science and Metallurgy, Cambridge CB2 3QZ, U. K.
Swiss Steel AG, Emmenbrücke, Switzerland

Abstract

Case hardening steels produced from continuous cooling processes often exhibit a multiphase microstructure. The parameters of the cooling process then define the product properties in cases where no additional annealing treatment is required. However, these steels can be very sensitive to process parameters. To optimise the properties after the cooling process is therefore not a trivial task. Using exclusively experimental methods can be costly in terms of the resources required. Computer modelling helps accelerate the development process.

A new mathematical scheme has been applied to estimate the complete microstructure of some traditional multiphase steels following continuous transformation of austenite. The predictions are compared with experimental laboratory-data as well as some industrial scale trials.

1 Introduction

Traditional case hardening steels are unalloyed or low-alloy steels with a typical carbon content of 0.15-0.20 wt% [1]. They are expected to have an initial microstructure which is a mixture of ferrite and pearlite, which in some applications is cold-headed or machined prior to carburisation at about 900°C and subsequently hardening. The surface of the component is then wear-resistant whereas the core remains tough and ductile. The properties required from the core determine the minimum steel hardenability. In components such as gears or diesel injection systems, it is necessary for the core to be strong as well as tough, so the final microstructures must be fine, usually tempered martensite.

If the microstructure (bainite, martensite *etc.*) and mechanical properties in the hot-rolled wire or bar are not as required, a heat-treatment is needed to ameliorate the problems and this accrues

additional costs. It would be useful therefore to obtain the desired features directly from the hot-rolling mill. As a result, Swiss Steel AG undertook a three stage research programme to investigate candidate alloys, involving the dilatometric measurement of continuous cooling transformation diagrams, laboratory-scale rolling experiments and industrial trials on a full-scale hot-rolling mill. Computer modelling can also play a role in this process and the experimental data generated can in turn serve to validate the theory. The purpose of the work presented here was therefore to compare calculations done using a recent microstructure model [2] against experimental data generated at Swiss Steel AG.

2 Dilatometry

As a starting point for determining the parameters for hot-rolling, continuous cooling transformation (CCT) diagrams were measured using dilatometry. This has the advantage that the small samples minimise temperature gradients and also permit a uniform austenite grain structure when compared with typical hot-rolled bars.

Cylindrical dilatometric samples of diameter 4 mm and length 7 mm were used on a push-rod *BÄHR DIL805* high-speed dilatometer with radio frequency induction heating was used. The sample temperature is measured by a thermocouple welded to its surface using a precision welder and jig supplied by the dilatometer manufacturer. The heating and austenitisation treatments were carried out under a vacuum of 5×10^{-4} mbar, and the cooling was achieved using helium or argon gas. As an illustration, the 50 nm resolution of the *BÄHR* dilatometer permits the measurement of a strain as small as 7.1×10^{-6} corresponding to a martensite volume fraction of 1.1×10^{-3} at 400°C [3].

The chemical composition of the steel is given in Table 1. Two different austenitizing temperatures were chosen to achieve austenitic grain sizes of $\bar{L} = 13 \pm 2 \mu\text{m}$ and $\bar{L} = 23 \pm 2 \mu\text{m}$ respectively, where \bar{L} is a mean lineal intercept. Before cooling the samples were given a 60% plastic reduction at the austenitisation temperature in the dilatometer; it should be noted that in the steel concerned the austenite grain structure recrystallises rapidly so the subsequent transformation occurs from equiaxed austenite of the size stated above. The cooling rates were in the range $0.2 - 6.0 \text{ K s}^{-1}$.

The resulting microstructures were measured using point counting and optical microscopy; the measured fractions typically have a statistical error of about $\pm 10\%$ of the absolute value. Furthermore, it was decided not to attempt to distinguish between bainite and martensite because of a lack of clarity. The experimental data are therefore presented as the combined fraction of bainite (α_B) and martensite (α'). Allotriomorphic ferrite, pearlite and Widmanstätten ferrite are labelled α , P and α_W respectively in the plots presented in Fig. 1. The calculations are all done using the theory described in the accompanying paper by Chen *et al.* [2].

It is evident from Fig. 1 that although there are detailed discrepancies, the comparison between experiment and theory for allotriomorphic ferrite and pearlite is reasonable. It should be borne in mind that there are experimental errors in making these measurements which are estimated at about $\pm 10\%$ of the absolute values of both phase fractions and austenite grain size. Nevertheless, and as expected, the fraction of both α and P decreases substantially as the cooling rate is increased.

Furthermore, less α and P is predicted and observed as the austenite grain size increases; this is because both of these transformations originate at the austenite grain surfaces and a smaller \bar{L}_γ provides a greater number density of nucleation sites.

The major difficulties arise in estimating the remaining phases. The calculations consistently indicated the absence of any bainite, although the calculated fraction of $\alpha_W + \alpha'$ correlates well with the measured fraction of $\alpha_W + \alpha'$. One possibility is that what is identified experimentally as bainite is in fact Widmanstätten ferrite, but this remains to be proved. Another possibility is related to the fact that the bainite model does not allow for cementite precipitation [2, 4]; the steel does not have sufficient silicon or aluminium to prevent the precipitation of cementite during the bainite reaction, Table 1.

These issues can be resolved both using transmission electron microscopy [5] and by studying the incomplete reaction phenomenon associated with the bainite reaction in this steel [5–9]. Furthermore, the evolution of microstructure as a function of time has not been displayed in Fig. 1 and this should be possible since both the dilatometric data and the computer model [2] present such time-resolved data. A detailed examination can then be made of transformation temperatures and available thermodynamic driving forces to check the mechanism of transformation [10]. These issues are reserved for work to be done in the near future.

C	Si	Mn	P	S	Ni	Cr	Mo	Al	Cu	N
0.17	0.19	1.20	0.01	0.023	0.076	1.05	0.008	0.022	0.125	0.009

Table 1: Chemical composition (wt%) of the steel used for dilatometric experiments.

3 Industrial trials

These trials were performed under regular production conditions at Swiss Steel AG. The molten steel produced in an electric arc furnace from scrap was cast continuously into 140×140 mm billets. They were then reheated to 1200°C and hot-rolled into wire rods or bars.

The plant trials were done under three different cooling conditions. As examples, the results from a 6.5 mm wire rod (Stelmor controlled cooling conveyor), a 23.5 mm wire rod (Garrett coiling line) and a 36 mm bar were described below.

At the Stelmor line the coil is pulled apart and each ring of the coil is treated under equal conditions. The covering of the line allows a slow and homogeneous cooling. For small diameters the cooling rate is not expected to vary much from the surface to the centre of the wire. The chemical composition of the steel is given in table 2. The cooling rate between 800 and 500°C as measured using a pyrometer is 0.34 K s^{-1} .

To determine the correct austenite grain size \bar{L} , sampling should be done just before the phase transformation starts. Under production conditions this cannot be done. Therefore a decision was made to cut samples at the shears just before the last hot deformation took place and to directly quench them into water. The grain size was then determined using optical microscopy (Fig. 2). It

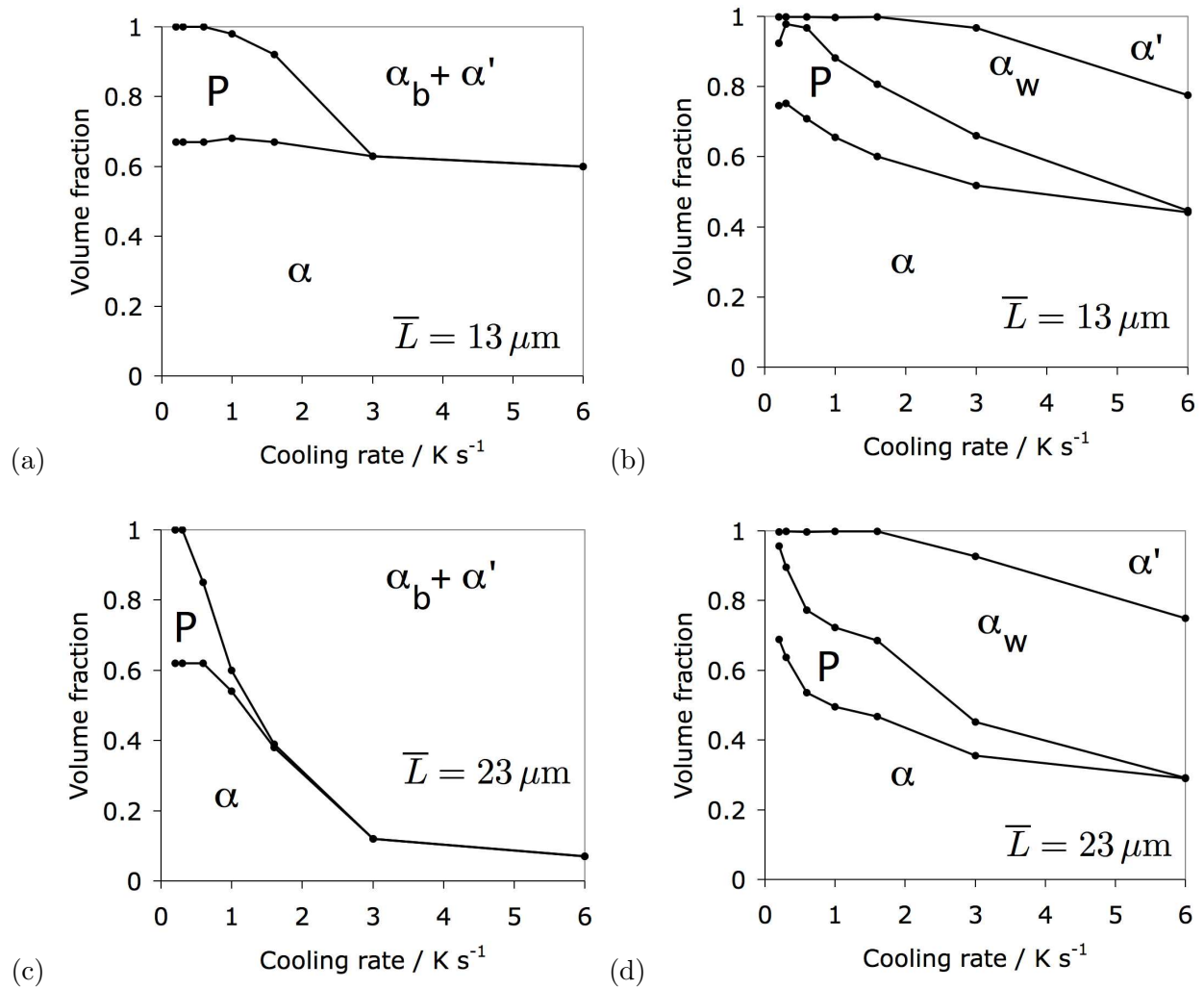


Figure 1: Measured (a,c) and calculated (b,d) microstructures for two austenite grain sizes.

C	Si	Mn	P	S	Ni	Cr	Mo	Al	Cu	Sn	N
0.16	0.21	1.21	0.009	0.026	0.13	0.98	0.015	0.037	0.30	0.016	0.0105

Table 2: Chemical composition (wt%) of steel used in the 6.5 mm Stelmor rolling trial.

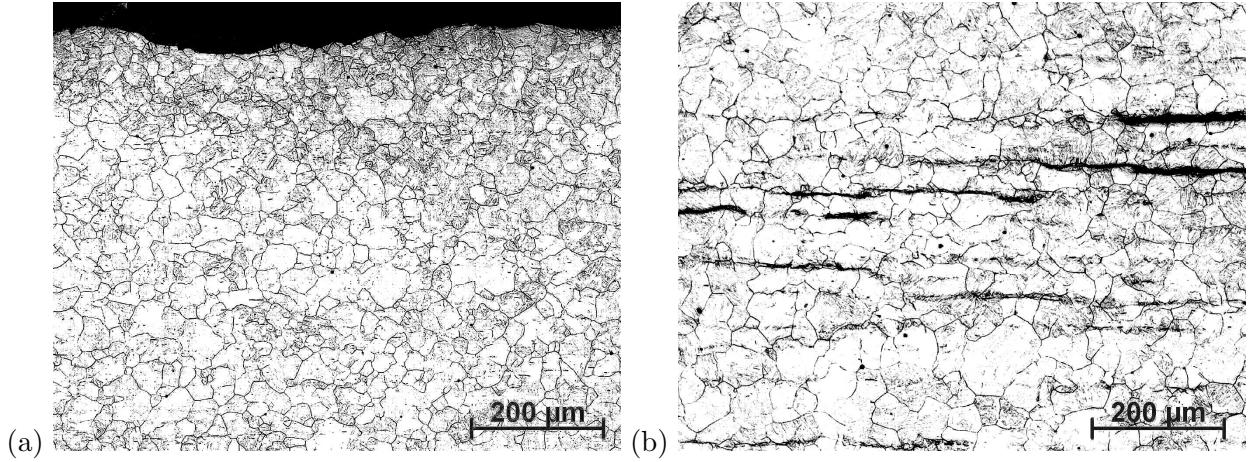


Figure 2: Austenite grain structure. (a) At the surface, (b) at the centre.

$\bar{L} / \mu \text{ m}$	V_{α}^e	V_{α}^c	V_P^e	V_P^c	$V_{\alpha_b}^e$	$V_{\alpha'}^e$	$V_{\alpha_w}^c$	$V_{\alpha_b}^c$	$V_{\alpha'}^c$
20.3	0.75	0.66	0.21	0.24	0.01	0.02	0.10	0	0
25.4	0.71	0.58	0.15	0.24	0.07	0.07	0.18	0	0
36.2	0.71	0.45	0.09	0.23	0.09	0.11	0.32	0	0

Table 3: Calculated and measured phase fractions on a 6.5 mm diameter rod cooled at 0.34 K s^{-1} . In V_{α}^e the superscript refers to an experimentally measured value whereas with V_{α}^c the superscript stands for a calculated value. This convention applies throughout.

was found to increase from the surface ($20 \pm 2 \mu\text{m}$) to the centre of the wire ($36 \pm 4 \mu\text{m}$).

The differences in the austenite grain size should lead to a change in the microstructure across the cross-section of the wire. Some encouraging comparisons are presented in Table 3 and Fig. 3.

The second trial was performed at the Garrett cooling line. In this case the wire is coiled directly after hot rolling leading to differences in the cooling rate between outer and inner rings within the coil. Such a compact coil cools very slow and the measured cooling rate was 0.16 K s^{-1} . The composition of the steel is given in Table 4.

C	Si	Mn	P	S	Ni	Cr	Mo	Al	Cu	Sn	N
0.20	0.19	1.23	0.008	0.031	0.11	1.00	0.017	0.027	0.19	0.010	0.0087

Table 4: Chemical composition (wt%) of steel used in the 23.5 mm Garrett rolling trial.

The sampling for the austenite grain size determination was done just after coiling with steel samples quenched into water; the size was found to vary from $26 \mu\text{m}$ at the surface to $50 \mu\text{m}$ at the centre of the sample. Due to the very low cooling rate, only a small quantity of bainite is formed at the core (Table 5). Fig. 4 shows that reasonable overall agreement is obtained even though there is not yet a detailed consistency between the contents of the measured and calculated “remaining phases”.

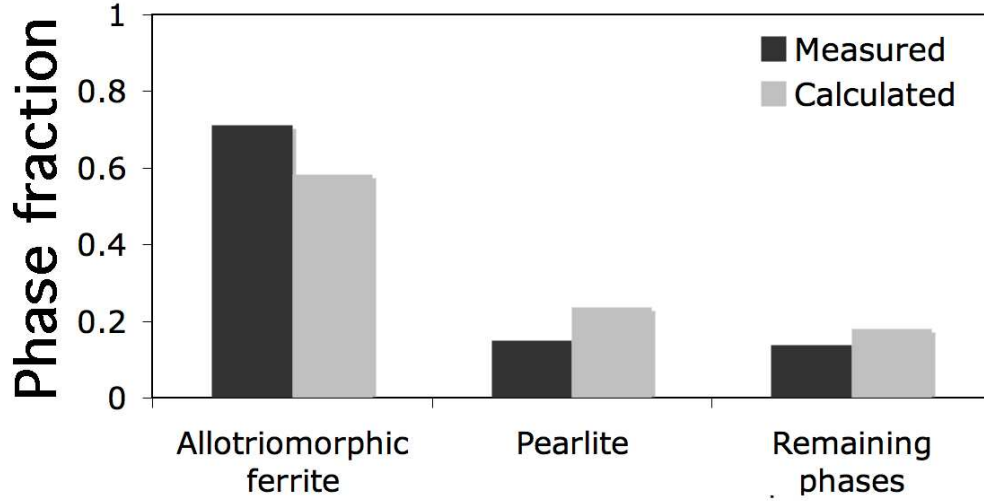


Figure 3: Calculated and measured phase fractions for the 6.5 mm diameter sample with an austenite grain size of $25.4 \mu\text{m}$

$\bar{L} / \mu\text{m}$	V_{α}^e	V_{α}^c	V_P^e	V_P^c	$V_{\alpha_b}^e$	$V_{\alpha'}^e$	$V_{\alpha_w}^c$	$V_{\alpha_b}^c$	$V_{\alpha'}^c$
26	0.66	0.64	0.35	0.32	0	0	0.03	0	0
31.8	0.57	0.58	0.41	0.32	0.02	0	0.10	0	0
49.5	0.78	0.42	0.22	0.32	0.01	0	0.26	0	0

Table 5: Calculated and measured phase fractions from a 23.5 mm diameter rod cooled at 0.16 K s^{-1} .

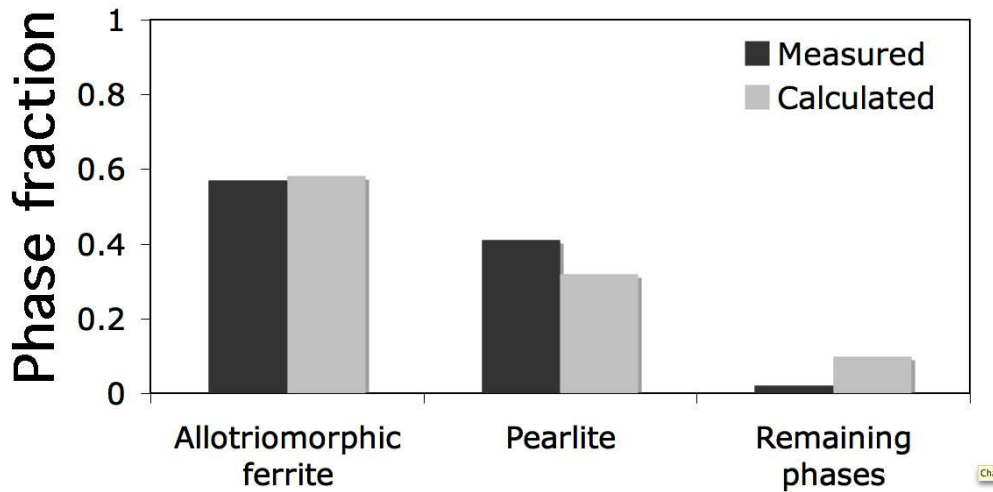


Figure 4: Calculated and measured phase fractions for the 23.5 mm diameter sample with an austenite grain size of $31.8 \mu\text{m}$.

Bar production was considered in the third and last trial. The modelling of a 36 mm bar is most challenging. The variation of cooling rates over the cross-section is more pronounced than in the former two cases leading to a larger gradient in the GS. The GS from samples taken at the cooling bed varies from 19 μm at the surface over 48 μm at mid-radius to 67 μm at the centre.

Due to the higher cooling rate of 0.8 K s^{-1} more bainite and martensite are formed. The bainite plus martensite contents are: 23% at the surface, 58% at mid-radius and 86% at the centre of the bar. Some comparisons are presented in Table 7 and Fig. 5.

C	Si	Mn	Ni	Mo	Cr	V
0.17	0.19	1.22	0.09	0.018	1.03	0

Table 6: Chemical composition (wt%) of 36 mm diameter bar.

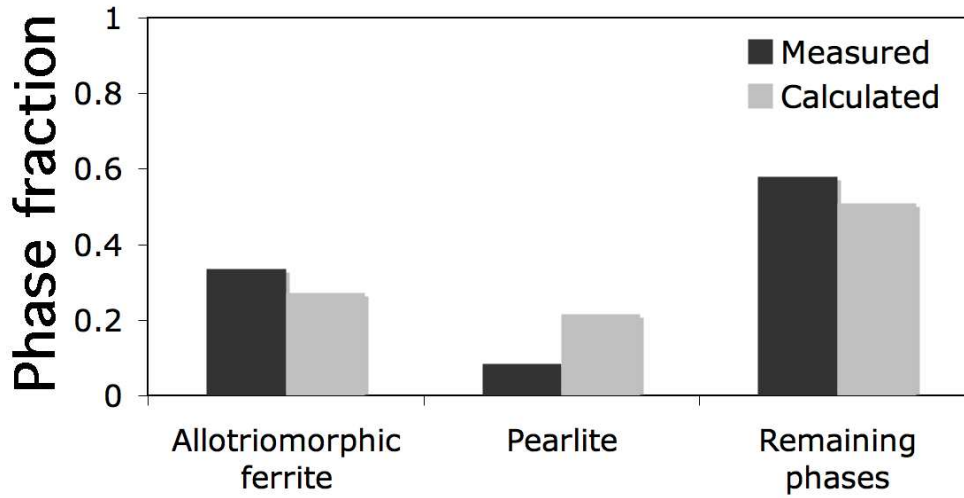


Figure 5: Calculated and measured phase fractions for the 36 mm diameter sample, with an austenite grain size of 47.8 μm .

4 Summary

It has been possible to apply a new computer model to both dilatometric data and some commercial trials. It has been demonstrated that the model reproduces trends, especially with respect to the

$\bar{L} / \mu\text{m}$	V_{α}^e	V_{α}^c	V_P^e	V_P^c	$V_{\alpha_b}^e$	$V_{\alpha'}^e$	$V_{\alpha_w}^c$	$V_{\alpha_b}^c$	$V_{\alpha'}^c$
19.3	0.48	0.56	0.29	0.23	0.23	0.22	0	0	
47.8	0.34	0.27	0.09	0.21	0.58	0.51	0	0	
66.9	0.13	0.20	0.02	0.21	0.86	0.58	0	0	

Table 7: Calculated and measured phase fractions from a 36 mm diameter rod cooled at 0.8 K s^{-1} .

reconstructive transformations (allotriomorphic ferrite and pearlite). However, there are detailed discrepancies between the predicted fractions of bainite, Widmanstätten ferrite and martensite when comparisons are made against measurements. Before reaching conclusions about these difficulties it is necessary to accumulate a better experimental dataset which is based on a rigorous and if necessary a higher resolution determination of the phases being characterised.

Acknowledgements

We are grateful to Swiss Steel for financing this work and to Professor A. L. Greer for the provision of laboratory facilities at the University of Cambridge.

References

- [1] S. Lampman. *Introduction to Surface Hardening of Steels*, volume 4, pages 259–267. ASM International, Materials Park, Ohio, USA, 1991.
- [2] J. Chen, H. K. D. H. Bhadeshia, S. Hasler, H. Roelofs, and U. Ulrau. Complete calculation of steel microstructure for strong alloys. In *New Developments on Metallurgy and Applications of High Strength Steels*, page in press, Argentina, 2008. Tenaris, Tenaris.
- [3] H.-S. Yang and H. K. D. H. Bhadeshia. Uncertainties in the dilatometric determination of the martensite–start temperature. *Materials Science and Technology*, 23:556–560, 2007.
- [4] H. Matsuda and H. K. D. H. Bhadeshia. Kinetics of the bainite transformations. *Proceedings of the Royal Society of London A*, A460:1710–1722, 2004.
- [5] H. K. D. H. Bhadeshia. *Bainite in Steels, 2nd edition*. Institute of Materials, London, 2001.
- [6] H. K. D. H. Bhadeshia and D. V. Edmonds. The bainite transformation in a silicon steel. *Metallurgical Transactions A*, 10A:895–907, 1979.
- [7] H. K. D. H. Bhadeshia and D. V. Edmonds. The mechanism of bainite formation in steels. *Acta Metallurgica*, 28:1265–1273, 1980.
- [8] P. G. Self, H. K. D. H. Bhadeshia, and W. M. Stobbs. Lattice spacings from lattice fringes. *Ultramicroscopy*, 6:29–40, 1981.
- [9] H. K. D. H. Bhadeshia and J. W. Christian. The bainite transformation in steels. *Metallurgical & Materials Transactions A*, 21A:767–797, 1990.
- [10] H. K. D. H. Bhadeshia. Rationalisation of shear transformations in steels. *Acta Metallurgica*, 29:1117–1130, 1981.